Dynamic comparison of different types of slab tracks and ballasted track using a flexible track model

J. Blanco-Lorenzo, J. Santamaria, E.G. Vadillo and **O. Oyarzabal**
Department of Mechanical Engineering, University of the Basque Country. Alameda Urquijo s.n., 48013 Bilbao, Spain.

DOI: 10.1177/0954409711401516

Please cite this paper as: **J. Blanco-Lorenzo, J. Santamaria, E.G. Vadillo and O. Oyarzabal,** *Dynamic comparison of different types of slab tracks and ballasted track using a flexible track model*. Proc. IMechE Part F: Journal of Rail and Rapid Transit, Vol. 225, pp. 574-592. 2011

Dynamic comparison of different types of slab tracks and ballasted track using a flexible track model

J. Blanco-Lorenzo[1], **J. Santamaria, E.G. Vadillo** and **O. Oyarzabal**
[1] Department of Mechanical Engineering, University of the Basque Country
Corresponding author: Alameda Urquijo s.n., 48013 Bilbao, Spain.
javier.santamaria@ehu.es

DOI: 10.1177/0954409711401516

Abstract: The dynamic performance of a ballasted track and three types of slab tracks is analysed and compared by means of a comprehensive dynamic model of the train-track system, generated using two commercial analysis software packages: the commercial Multibody System (MBS) analysis software SIMPACK and the Finite Element Method (FEM) analysis software NASTRAN. The use of a commercial MBS software makes it possible to include in a reliable way models of advanced non-linear wheel-rail contact, as well as complex elements or joints in the vehicle model, while the FEM the flexibility of the rail and the slab to be taken into account. As a result, a combined MBS-FEM representation of the vehicle-track model is integrated into the MBS software, which allows for the study of dynamic phenomena in a wide frequency range. In this work, other simpler approaches for modelling the dynamic vehicle-track interaction are also considered, such as pure Multibody or Finite Element representations of the whole vehicle-track system. The quality of the results obtained with the different types of models used is analyzed, and some conclusions are put forth regarding the possible validity of rather simple train-track interaction model types under certain conditions as well as the most suitable configuration of the most complex models.

1. INTRODUCTION

Ballast has been used since the beginning of railways in order to serve as the transition element between the sleepers and the soil, providing compliance, and vibration damping, as well as surfacing and draining capabilities to the track. The increased maintenance costs and reduced life cycle of the track associated with higher transportation speeds, axle loads and traffic densities led to the appearance of the slab track in the 1960s.

Some of the advantages of the slab track with respect to the ballasted track are its higher geometric stability and reduced maintenance costs, as well as easier access to the track and evacuation thanks to the absence of blocking elements between the rails. The main disadvantage of the slab track is its higher installation cost. Apart from that, railway administrations and design engineers often prefer to use traditional ballasted track designs instead of newer slab track designs, because much more experience has been collected with the use of the former track type.

Within the different slab track types, floating slab tracks provide an effective way to reduce vibration transmission from railway traffic to the ground [1-3]. By adding an elastic layer beneath the slab, the natural frequency of the system is reduced, at the expense of increasing its cost.

In this work, the dynamic performance of the ballasted track and three different types of slab tracks is compared. In two of the slab track types considered, the slab is directly supported on the soil (in one of them there is a single elastic level above slab, and in the other there are two elastic levels above slab), and

in the third one, the slab is isolated from the soil by means of an elastomeric mat (i.e. it is a floating slab track).

The main parameters that are considered to evaluate the dynamic performance of each of the studied track types are: a) the vertical wheel-rail contact force, which is relevant in relation to rail bending fatigue and rolling stock deterioration at low and mid frequencies, and in relation to short-pitch corrugation growth and rolling noise generation at higher frequencies; and b) the vertical pad force, which is relevant to the pad life and fastening system fatigue.

A comprehensive multibody model of the train-track system, in which the rails and slab of the track are incorporated as flexible bodies, and which includes an advanced non-linear wheel rail contact model, has been used to study the vehicle-track dynamic interaction. The model has been constructed within the commercial MBS code SIMPACK, in combination with the use of the FEM analysis package NASTRAN.

Until rather recently, standard tools enabling integrated MBS-FEM systematic modelling could not be found in commercial MBS or FEM analysis packages, mainly due to the relatively high computational costs involved. Traditionally, when there has been a need for models capable of considering the dynamic interaction between vehicle and track in a representative way, they have been developed exclusively by the interested research teams, tailored for each specific study. Many examples of this can be found in the literature (see for example refs. [4-8]) and comprehensive surveys of the current practice and state-of-the art, can be found in [9] and [10]. Detailed discussions on the vehicle and track modelling are provided in [11] and [12], and on the utilization of FEM analysis for track models in [13]. [14] also provides a useful overview of the problem, and summarizes the options available within commercial railway vehicle MBS codes, including the most advanced which have appeared in recent years. Refs. [14-16] show some interesting application examples in which multibody models including elastic bodies are used. ADAMS Rail is used as the analysis software in refs. [14] and [15], and SIMPACK in ref. [16].

Other simpler types of vehicle-track models have been also considered in this work in order to simulate the vehicle-track dynamic interaction. One of the simpler model types that has been used is a pure multibody model, in which the track is represented by means of a set of discrete mass, spring and damper elements placed beneath each of the vehicle's wheelsets. The other type of simpler model is a pure FEM model, in which the relative displacement between vehicle and track is neglected (i.e. the vehicle is stationary with respect to the track, and the rail irregularity is moving), and the wheel-rail contact condition is simplified to a linear spring.

The first type of model (i.e. the multibody model with elastic bodies to represent the rails and the slab) is the one which offers the most realistic representation of the vehicle-track system, and also the one which involves the highest computational costs. However, as it will be shown in following sections, in some situations the simpler pure multibody or FEM models may be capable of producing comparable results. Apart from comparing the dynamic performance of the different track types considered, in this work the results obtained with the different types of models used are also compared, and the reasons for the validity of the simpler types of models under certain conditions are discussed.

2. DESCRIPTION OF THE STUDIED TRACK TYPES

Four track types have been considered in the studies presented here: the traditional ballasted track, and three types of slab tracks: the RHEDA 2000 track, the STEDEF track, and a floating slab track. The relevant parameters that have been used in the simulations for each track type are the usual parameters of new high performance tracks in Europe, and are given in Table 1.

It has to be mentioned that the values of the physical parameters of the tracks considered in the simulations are typical values based on standard configurations of each type of track, and may vary within a certain range. Consequently, the results and conclusions presented in this work must not be considered as absolute statements or extended straightforwardly to other possible configurations of each type of track.

In all cases, the modelled tracks are considered to rest on an infinitely stiff soil.

The parameters chosen for the ballasted track correspond to a high performance ballasted track adequate for high speed traffic.

In Table 1 the sleeper support vertical stiffness and relative damping refer to the properties of the elastic level below the sleeper, i.e. the ballast for the ballasted track, and the elastomeric material above which each sleeper rests in the STEDEF track.

As for the rail properties, a UIC-60 rail section is considered in all cases. The mechanical properties of the rail material and the geometric properties of the rail section are the same as those given in [4].

Table 1 Parameters of the different track types considered in the simulations

Parameter	BALLAST	RHEDA 2000	STEDEF	FLOATING SLAB
Rail pad vertical stiffness [kN/mm]	100	24.6 (*)	150	213.2
Rail pad vertical (relative) damping [kNs/m] or [%]	15	10% (**)	10%	14.8
Sleeper mass [kg]	320	138	221.7	-
Rail support spacing [m]	0.60	0.65	0.60	0.60
Sleeper support vertical stiffness [kN/mm]	100	-	50	-
Sleeper support vertical relative damping [%]	20%	-	10%	-
Slab cross section dimensions (width*height) [m]	-	3.2*0.24	2.9*0.49	2.5 x 0.55
Slab support stiffness per unit area [kN/m^3]	-	-	-	15000
Slab support damping per unit area [kNs/m^3]	-	-	-	30
Slab concrete Young's modulus [GPa]	-	34	29	30
Slab concrete shear modulus [GPa]	-	14.2	12.1	11
Slab concrete density [kg/m3]	-	2500	2500	2500
Slab concrete relative viscous damping [%]	-	1%	1%	1%

(*) Combined stiffness of the upper rail pad and lower base plate pad in series. The stiffness values for each of the two pads are 450 kN/mm and 26 kN/mm respectively.
(**) For both the rail pad and the base plate pad.

Figure 1 shows the dynamic models of the different types of track studied, and in the following sections a brief description of the three studied slab track types is given.

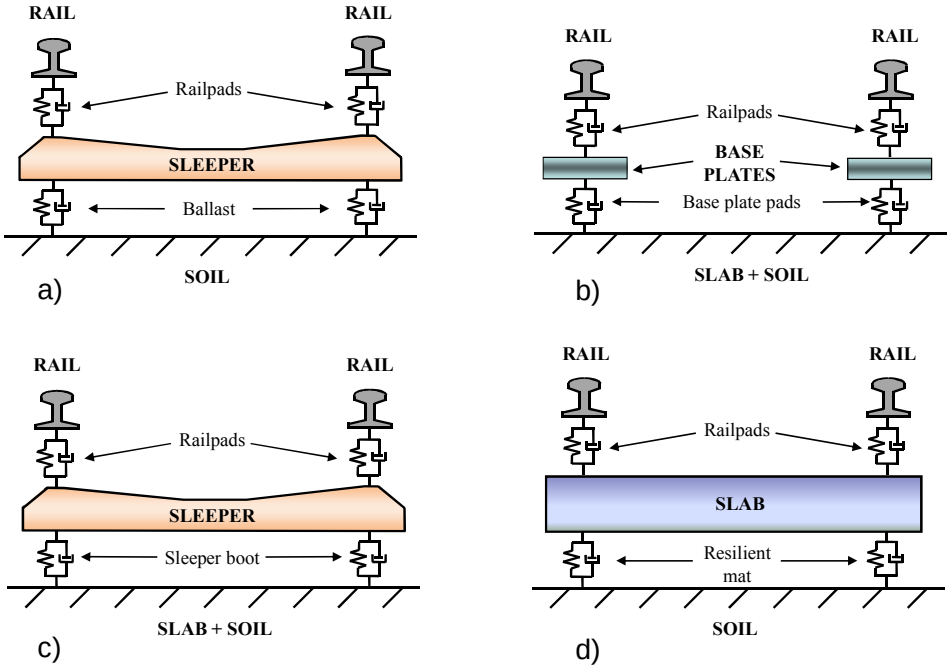

Fig. 1 Cross sections of the dynamic models of the ballasted track (a), the RHEDA 2000 track (b), the STEDEF track (c), and the floating slab track (d).

2.1 RHEDA 2000 track

This is the type of slab track that has been most used in Europe. The rails are discretely supported above each sleeper, and the sleepers are directly embedded in the slab, forming a monolithic assembly. Therefore, most of the vertical flexibility and damping of the track is provided in the rail fastening system, which is usually of the type VOSSLOH IOARV 300 [17]. This fastening system comprises two elastic levels: one is given by the rail pad, located between the rail and the base plate, and the other by the base plate pad, located between the base plate and the sleeper. Therefore, for modelling this track two elastic layers are considered between the rails and the slab. The base plate has a mass of 4.4 kg.

The reinforced concrete slab of this track is continuous, and is executed on the field. The slab rests on a layer of gravel and cement or lean concrete, which are materials of very high stiffness compared to the elements in other elastic levels of the track; therefore the slab can be considered directly supported on the soil with no elasticity beneath it (i.e. the slab does not vibrate).

2.2 STEDEF track

In the STEDEF slab track there are two elastic levels above the slab. One, like in the other track types studied, is given in the rail fastening system, and in this case the rail is also discretely supported above each sleeper. Different options are available for the rail fastening system, the simplest being the NABLA type. This fastening system has a single elastic level.

The second elastic level above the slab is given between the sleepers and the slab, since these are not directly built into the slab like in the RHEDA 2000 track, but they rest above an elastomeric material.

As in the case of the RHEDA 2000 track, the reinforced concrete slab of the STEDEF track is continuous, and executed on the field. In this case again, the slab rests on a layer of gravel and cement or lean concrete, and no elastic level is considered beneath it.

2.3 Floating slab track

The application of floating slab tracks is mainly focused to reducing vibration transmission from railway traffic to the ground [1-3]. The slab is isolated from the ground by means of a resilient layer, which may consist of single support bearings, steel springs, or of a continuous elastomeric mat. Therefore, unlike in the other two types of slab tracks previously described, in this type of track an elastic layer is considered beneath the slab.

By maximizing the resilience of the elastic layer beneath the slab, the cut-on frequency of the system is reduced, and a more effective reduction in the transmission of vibrations to the ground can be achieved. The slab mat resilience, however, is limited by the maximum allowable static rail deflection [1].

Above the slab, the track has a single elastic level, given by the discrete support pads between the rails and the slab.

The parameters chosen for this track are taken from ref. [1]. These parameters correspond to a stiff pad for the rails, and soft mat for the slab. This combination of parameters can be adequate to reduce wheel-rail force and track deflection, to ensure riding quality and train stability and to reduce force transmission to the subgrade due to environmental concerns [3].

3. DESCRIPTION OF THE VEHICLE-TRACK INTERACTION MODELS

Sometimes, rail vehicle dynamic studies are carried out by means of rather simple multibody models of the vehicle, neglecting the track's elasticity. Examples of case studies where such models can be valid include ride comfort analysis, and vehicle curve inscription analysis.

In the case of ride comfort analysis, the dynamics of the sprung masses of the vehicle are of primary interest, and these are uncoupled from the track dynamics by means of the primary and secondary suspensions. In the case of curve negotiation analysis, the dynamics of the vehicle's axles normally occur at frequencies too low for the track to be excited dynamically, and thus they are determined by the vehicle's dynamic properties, but not by the track's. However, such analyses are only valid for very low frequencies, normally below around 20 Hz, where the track behaves as a relatively stiff spring [9,11,12]. When phenomena at higher frequency ranges need to be studied, consideration of the track elasticity becomes mandatory.

In this work, different types of models for the study of vertical vehicle-track dynamic interaction in the time domain, which account for the elasticity of the track, have been constructed combining the use of a commercial FEM software (NASTRAN) and a commercial MBS software (SIMPACK), following three different approaches as explained below.

3.1 Rigid Multibody (RMB) train-track interaction models

This is the simplest approach to model a vehicle-track interaction model in a MBS environment, and is the standard option which is available in some MBS analysis programs, including SIMPACK, for modelling an elastic track.

The idea consists of employing discrete elements of mass, stiffness and damping for modelling the different elastic levels of the track, in a similar way as is done for the vehicle. A group of lumped mass, spring and damper elements are placed below every axle of the vehicle, each of those groups always remaining below the axle to which is associated (see [14] for example). Therefore, each of those groups travels along the running path of the vehicle at the same speed as each of the vehicle's axles.

The physical parameters of mass, stiffness and damping assigned to each lumped element beneath the vehicle's wheelsets are found in this work by adjusting the vertical receptance of the mass-spring-damper assembly beneath each wheelset to that of the track, the latter being calculated in a frequency analysis with a FE model of the track.

With a proper adjustment of the parameters of the discrete assemblies beneath each wheelset, a quite good correspondence between the receptance of the track calculated with a FEM model and the receptance of the discrete assemblies can be achieved, at low and mid-frequencies up to a few hundred Hz. Figure 2 shows as an example the adjustment of receptances achieved for the ballasted track.

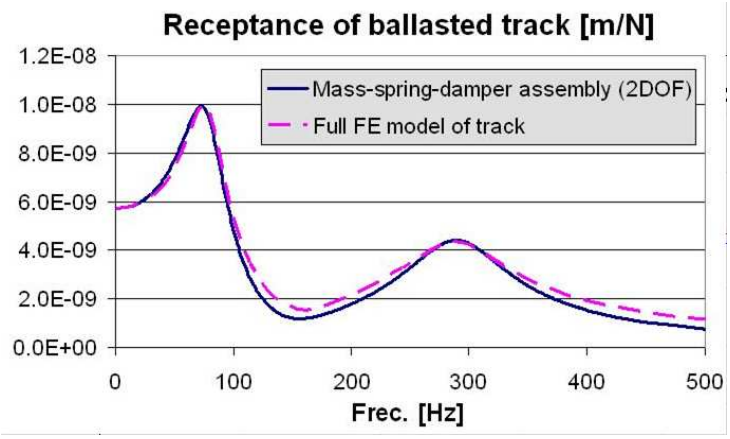

Fig. 2 Comparison of the modulus of the receptance of the ballasted track calculated with a FEM model of the track, with the receptance of the equivalent discrete mass-spring-damper assembly of the track beneath each of the vehicle's wheelsets.

The real behaviour of the longitudinally continuous elements of the track, namely the rails, and if it is the case, also the slab, cannot be properly represented with this type of model. The possible effect in the vehicle-track interaction of the rail bending between two consecutive sleepers in the case of discretely supported rails is also neglected. It has to be mentioned as well that local characteristics/imperfections in the track, such as voided sleepers, cannot be properly dealt with.

The contact condition between wheel and rail is achieved with the standard wheel-rail pair available in the SIMPACK Rail environment [18]. An hertzian contact model is used, with the possibility of multiple contact patches in the same wheel-rail pair. In this work, the tangential forces and torque in each contact are calculated with the FASTSIM algorithm, with a discretization of the contact patch of 11*11 elements.

A full 3-D model of the vehicle with 50 DOF, and a simplified model consisting of a single wheelset with a static force applied into it, have been used with this type of train-track interaction model, to obtain the results show in sections 5 and 6.

3.2 Finite element (FE) train-track interaction model

In this type of model, both train and track are completely modelled in a FE environment. The elements used for modelling the different components of the track are similar to those used in the Elastic Multibody vehicle-track models, which are described in the next section: BEAM elements are used for the rails, lumped linear viscoelastic elements for each railpad, sleeper support, and flexible material beneath slab, lumped masses for each sleeper, and one-dimensional BEAM or solid HEXA elements for the slab.

The vehicle is modelled by means of lumped mass, spring and damper elements. A model of a quarter of the vehicle has been considered, consisting of three elastic levels (wheelset, bogie and car body). The vertical displacement is the only degree of freedom in each elastic level. As a variation to this single wheelset model, a model of two wheelsets has also been used, consisting simply of two of the assemblies described here for the single wheelset model, separated by the bogie wheelbase distance. With this second model, the possible effect of wave reflections between different wheelsets of the vehicle can be studied.

These wave reflections can have a considerable effect on the wheel-rail contact forces, particularly at frequencies corresponding to vibration modes of the track with the rail vibrating with two, three and upper multiple half-wavelengths between the two bogie's wheelsets [9].

The contact between vehicle and track is accomplished by means of a linear BEAM element, which provides stiffness only in the vertical direction. The normal contact law is linearized according to the following equation:

$$k_H = \left.\frac{dN}{dz}\right|_{N=F} = \frac{3}{2} \times C_H{}^{2/3} \times F^{1/3} \tag{1}$$

Where k_H is the linearized contact stiffness, N is the normal wheel-rail force, F is the reference normal wheel-rail force, taken as the wheel-rail force in static conditions, and C_H is the Hertzian contact constant.

The FE models of vehicle and track are fully linear. Therefore, possible non-linear effects in the vehicle-track system, like wheel or sleeper lift-off, and non-linear characteristics of vehicle or track components, are not taken into account. However, it has been checked that with the level or excitation used in the simulations, wheel or sleeper lift-off does not occur. With a considerable increase in computation costs, it would be possible to include non-linear characteristics in these FE vehicle-track models which have a number of DOF at least one order of magnitude higher than the other two types of multibody vehicle-track models that have been used.

This type of vehicle-track interaction model is a moving irregularity model, since the vehicle remains static with respect to the track, while a strip of irregularity passes between wheel and rail. The irregularity is entered by means of a temperature excitation in the BEAM element that represents the vertical contact stiffness between wheel and rail: the rail irregularity at each point in time is converted to a temperature value, so that the thermal expansion of the BEAM element matches the desired value of rail irregularity.

This type of model is simpler to build than the elastic multibody (EMB) vehicle-track models that are described in the next section, and, since it is a linear model, its computational costs are considerably lower than in the EMB vehicle-track models, despite the higher number of DOF. Particularly, considerable savings in computation times are achieved thanks to the substitution of the sophisticated contact algorithm inside the MBS models, which calculates both the contact position and the contact forces in a non-linear way, by a simple linear spring between two fixed nodes. In addition, the track can also be represented with a high level of detail.

However, with FE models some capabilities with respect to the EMB vehicle-track model described in the next section are lost. Firstly, this model can only be used for the study of vertical dynamics, because wheel-rail contact pairs, necessary to properly account for the tangential forces at the wheel-rail interface, cannot be introduced (the contact condition is simplified by a linear spring). Additionally, the possible effect of the parametric excitation resulting from the varying dynamic stiffness of the track at different points along each sleeper bay is dropped out of the analysis, since the vehicle remains stationary at one given position on the track. Lastly, the same fact of the vehicle being stationary instead of moving with respect to the track, gives rise to another source of error: the rail vibration that reaches a moving wheel is not the same as the one that reaches a stationary wheel. This error is negligible if the wave propagation speed on the track is much higher than the train speed [4], but it can be important if the two speeds are of the same order.

3.3 Elastic Multibody (EMB) train-track interaction models

These are the most comprehensive vehicle-track interaction models that have been built in this work. Like in the RMB train-track models, SIMPACK is the main modelling environment for constructing the models. The models of the vehicle are also the same as in the case of the RMB models. The track models are more realistic than in those models, since this time continuous elastic bodies, instead of discrete elements, are used. In addtion, the relative longitudinal motion of the vehicle with respect to the track is properly taken into account, because the track doesn't travel together with the vehicle as in the RMB models, and the vehicle is not stationary at one point on the track, as in the FEM models. SIMPACK provides two main modules to integrate elastic bodies into MBS models, which are named FLEXBODY and FLEXTRACK. FLEXTRACK is oriented for the study of vehicle-track interaction at very low frequencies, e.g. the dynamic interaction of a vehicle with a flexible bridge structure, and it has been checked in this work that it is not adequate to reproduce dynamic phenomena at higher frequencies. Therefore, in this work FLEXBODY has been used to construct the EMB vehicle-track models; and here the procedure followed to build the models with this module is explained.

By means of FLEXBODY, the rails and slab of the different tracks are represented as elastic bodies inside the EMB vehicle-track models. Each elastic body is represented within the MBS model by means of a number of its natural modes, obtained in a previous real eigenvalue modal analysis of a FE model of the elastic component. In this case, NASTRAN has been used as the FE processor to perform the required modal analyses.

The output results of the modal analysis imported into the MBS model are the stiffness and mass matrices of the elastic track component, as well as its mode shapes. The dynamic behaviour of the elastic component is represented by means of modal superposition; i.e. each of the considered mode shapes of the elastic component is an additional DOF in the MBS model, and the equation of motion governing each of these DOFs is the uncoupled dynamic equation corresponding to that natural mode. For the case of an elastic rail, the equation of motion for the *i*th mode can be written as follows:

$$\ddot{z}_i(t) + 2\xi_i\omega_i\dot{z}_i(t) + \omega_i^2 z_i(t) = \frac{1}{m_i}\left[\sum_{j=1}^{m} f_{wr,j}(t)\Phi_i(x_{w,j}) - \sum_{k=1}^{n} f_{p,k}(t)\Phi_i(x_{p,k})\right] \tag{2}$$

where $z_i(t)$ is the modal displacement of the *i*th mode, ω_i its natural frequency, m_i its generalized mass, ξ_i its damping ratio, and $\Phi_i(x)$ its shape function. $f_{wr,j}(t)$ is the wheel-rail force at the *j*th wheel, $x_{w,j}$ the longitudinal location along the rail of the *j*th wheel, and *m* the number of wheelsets; $f_{p,k}$ is the force of the *k*th railpad, $x_{p,k}$ the location of said railpad along the rail, and *n* is the total number of railpads in the rail.

The movement of the elastic rail is described by superposition of the movements of the q modes describing its elasticity:

$$u_R(x,t) = \sum_{i=1}^{q} z_i(t)\Phi_i(x) \tag{3}$$

where u_R describes the movement of one of the degrees of freedom of the elastic rail as a function of the longitudinal coordinate *x* and time *t*. A similar equation can be written for each of the degrees of freedom of the rail (in the case of vertical vibration only vertical displacement and pitch rotation are relevant).

In this way, a compact and efficient representation of the elastic component within the MBS model is achieved, with comparatively few DOF (the considered normal modes of the elastic component). In order to increase the efficiency of the elastic body representation in the MBS model, it is convenient and often necessary to use some condensation technique in the FE model, so that the size of the mass and stiffness matrices and the eigenvectors that will be imported into the MBS model can be reduced to an extent that will make it possible for the MBS integration algorithm to handle them. It has to be taken into account that while FE codes can handle models with up to some hundreds of thousands of DOF, the size of MBS models is much more limited, typically up to some few hundred DOF.

For these purposes, the Generalized Dynamic Reduction (GDR) available in NASTRAN [19] has been used. It has been checked that this condensation method improves the results obtained with the static Guyan condensation [20], and that the error in the calculation of normal modes derived from the condensation step is small.

As will be discussed in the next section, both the number of modes and number of nodes of the condensed model of each elastic component necessary have been studied to obtain reasonable accuracy in its representation inside the EMB train-track models.

Concerning the coupling between vehicle and track, the standard wheel-rail pair element available in the SIMPACK Rail module is used here again, but this time some additional auxiliary elements need to be defined. The reason is that the wheel-rail pair element can only be defined between rigid bodies with no relative longitudinal motion, and the rails are modelled in this case as elastic bodies that do not travel along the track with the wheels.

The additional elements defined are: one moved marker in the elastic rail bodies for each of the vehicle's wheelsets, one dummy rigid rail body for each wheel-rail pair, and one kinematic constraint for each dummy rigid rail body. Figure 3 shows a schematic cross-section of this type of track model, describing the different elements used and their arrangement. In this figure a side view of the train-track interaction model is also depicted, in which the described auxiliary elements are omitted, and one bogie of the vehicle and the wheel-rail contact elements are added.

The moved markers move along each elastic rail, their longitudinal motion being defined with the longitudinal motion of the wheelset to which they are associated, and their vertical motion being defined by linear interpolation of the vertical displacements and pitch rotations of the two nearest interface nodes defined in the elastic rail.

The dummy rigid rail bodies also move along the track together with each of the vehicle's wheels, and their only purpose is to contain the rail profile geometry and to transfer the load from each wheel to the rails, serving as the Rail body in each wheel-rail pair. They are given a negligible mass, so as not to alter the dynamic properties of the track.

Lastly, the kinematic constraints are used to link the vertical displacement of each dummy rigid rail body to that of its corresponding moved marker. There is another option to couple the dummy rail bodies with the moved markers in the flexible rail, by means of stiff springs [16]. In order not to alter the dynamic properties of the model, a high value for the stiffness of this spring should be used. However, the high stiffness value of these springs, together with the low mass of the dummy rail bodies, introduces high frequency oscillations in the simulation, and compromises the stability of the numerical time step integration process. These problems are avoided using the mentioned kinematic constraint as is done in this work.

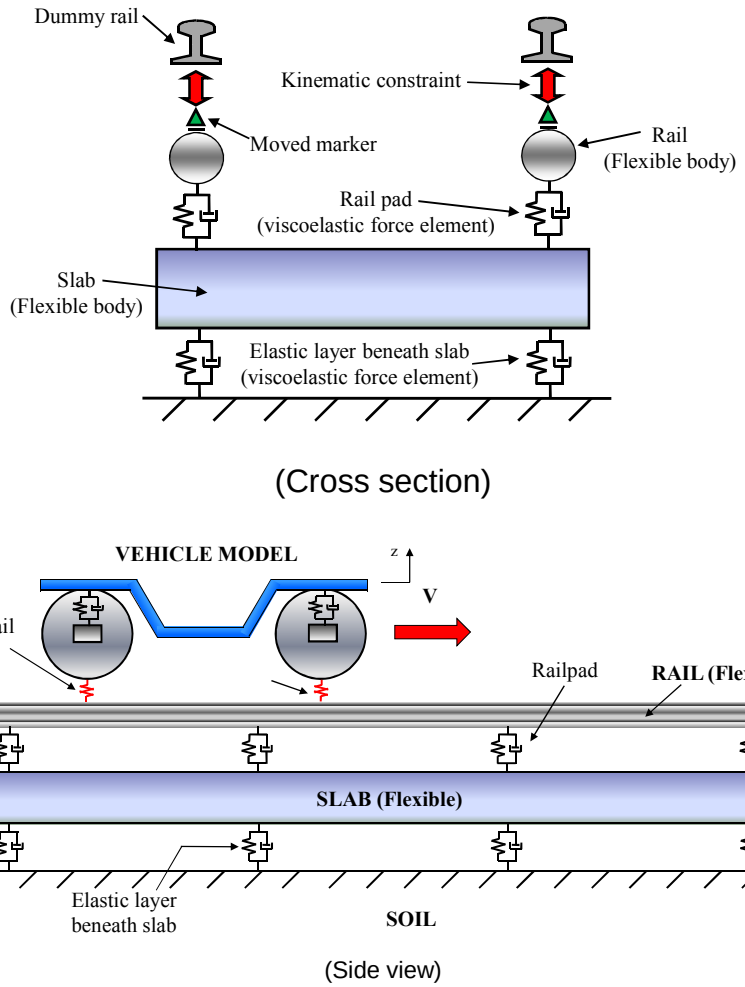

Fig. 3 Side view and cross section of the EMB model of the track, containing both elastic bodies and lumped elements (only one bogie represented in the side view)

The damping for each elastic body of the track is introduced by means of modal damping for each of the considered natural modes of the elastic component. As each elastic body is modelled separately, lumped force elements representing the concentrated stiffness and damping provided in each of the track's discrete supports (i.e. railpads, sleeper supports and ballast) can be defined between the different track bodies. Thus, the non-uniformly distributed and hence non-proportional stiffness and damping properties of a discretely supported track can be adequately modelled, without the need for a complex eigenvalue modal analysis.

Lastly, one limitation present in the EMB vehicle-track interaction models pertains to the length of flexible track simulated. While in the case of the previously described RMB vehicle-track models the length of simulated elastic track is unlimited, here a finite length of elastic track has to be considered, in order to limit excessive computational costs. The spurious effects from the boundaries can affect the

quality of the results in the middle of the track [21]. The approach to eliminate those spurious effects is simulating a sufficient length of track. In the simulation results presented here, track lengths up to 200 sleeper bays have been considered.

In the following paragraphs the modelling of each individual component of the track is explained in more detail. Since computational costs can become very high in this kind of models [14], it is necessary to exercise proper judgement in defining the degree of detail that is going to be considered in each component of the model, in order to achieve a reasonable precision-cost relationship. For this purpose, different options, with varying degree of complexity, have been considered for representing the elastic bodies inside the EMB vehicle-track models, as explained below.

3.3.1 Rails

The rails are modelled as continuous elastic bodies by means of one-dimensional finite element models, based on Rayleigh-Timoshenko beam elements. This model allows for a reasonably good representation of the vertical dynamic rail properties up to 2.5 kHz [12]. If lateral dynamics were to be considered, a more detailed representation of the cross section of the rail could be necessary, since the level of the rail cross-section distortion in the lateral vibration modes is much higher than in the vertical vibration modes [9,12].

The finite element models of the rails contain 12 to 24 beam elements per sleeper bay, although the model is reduced by condensation. The number of chosen nodes for the condensed model depends on the frequency of the upper natural vibration mode of the rail that needs to be considered: with increasing natural frequencies, more nodes per sleeper bay need to be taken in the condensed model, in order to be able to calculate the higher modes with little error. In the condensed models, at least the nodes above each sleeper position need to be taken (i.e. 1 node per sleeper bay), in order to serve as connection points for the railpads. If more nodes need to be incorporated in the condensed model, these nodes should be taken equidistant, because in this way the error in the calculation of eigenmodes with the condensed model is minimized.

When calculating the rail's eigenmodes, no intermediate support in the finite length of rail modelled is considered, only simple supports are defined as boundary conditions in each of its two ends. In order to represent adequately in the EMB vehicle-track models the dynamic behaviour of the rail under the influence of the multiple supports existing along its length, on the basis of the eigenmodes calculated for the rail without intermediate supports, the wavelength of the upper eigenmode considered has to be sufficiently small. As a consequence, a large number of eigenmodes need normally to be imported into the MBS models (the more eigenmodes the longer the distance of flexible track modelled).

The parametric excitation in tracks with discretely supported rails, resulting from the difference in the dynamic track stiffness between different positions along each sleeper bay, may have a significant effect in the wheel-rail contact forces (see [4] for example). The difference in the dynamic track stiffness arises from the rail bending between supports, and the wavelength of the upper eigenmode considered should be in the order of twice the sleeper distance at most, in order to be able to properly account for this rail bending between supports. The resulting eigenfrequency of the upper vibration mode considered may be much higher than the upper frequency of interest in the analysis. As importing a large number of eigenmodes in the MBS models can entail a considerable rise in computational costs (it has to be remembered that each of the imported eigenmodes for the elastic bodies represents one more DOF in the MBS models), the upper frequency of the necessary eigenmodes for the rail in order to obtain reasonable precision in the frequency range of interest has to be properly chosen.

3.3.2 Discrete supports and sleepers

Each discrete rail pad and sleeper support in the track models is modelled as a lumped viscoelastic element. The sleeper supports represent the stiffness and damping of the ballast beneath each sleeper in the case of the ballasted track, and the stiffness and damping of the elastomeric material between the slab and each sleeper in the case of the STEDEF track. The elastomeric mat beneath the slab is also represented by means of discrete independent viscoelastic elements in the case of the floating slab track.

Even though a considerable degree of non-linear behaviour is typically observed in these elastomeric elements, with stiffness values changing with preload level and frequency of excitation, the assumption of linear stiffness and damping properties is considered sufficient for the purposes of this study. Another possible source of non-linearity within the track may come from the possibility of sleeper lift off. However, it has been checked that with the level of vertical excitation used in the simulations, this does

not occur. Nevertheless, it has to be noted that in this type of model, non-linear stiffness and damping properties depending on the load level can be assigned to each support, if desired.

Each sleeper is modelled as a lumped rigid mass, with one degree of freedom (vertical displacement). In the case of the RHEDA 2000 track, the base plates in each of the rail supports are also modelled as lumped rigid masses.

3.3.3 Slab

The slab is modelled as a continuous elastic body, like the rails. Two types of meshing have been considered for this element: a) a 3-D meshing, using HEXA8 solid elements, and b) a 1-D meshing, similar to that used for the rails, using BEAM2 elements. With a 3-D mesh, the possible two dimensional vibration of the slab can be accounted for, as it is done in [8]. In many other references, a 1-D representation of the slab similar to the one proposed here is used, see for example [1-3].

As in the case of the rails, no support condition is considered beneath or above the slab when calculating its eigenmodes. In the case of the 3-D meshed slab models, a large number of nodes need to be considered in order to adequately calculate and represent the 3-D vibration modes of the slab. On the contrary, in the case of the 1-D meshed slab models, the number of needed nodes is much lower, as only one dimensional vibration modes are calculated. Additionally, the number of calculated eigenmodes for a given frequency range is lower than in the 3-D meshed slab models, as only the longitudinal vibration modes are considered in the analysis.

4. VEHICLE MODEL DESCRIPTION AND SIMULATION SET UP

The railway vehicle considered in the simulations is the high speed ICE 3 passenger car. Some of the physical parameters for the vehicle used in the simulations are given in Table 2.

Table 2 Parameters of the ICE 3 high speed vehicle.

Parameter	Value
Carbody mass (unloaded condition) [kg]	53500
Bogie mass [kg]	3500
Wheelset mass [kg]	1800
Wheel nominal rolling radius [m]	0.46
Bogie spacing [m]	17.325
Bogie wheelbase [m]	2.5

The vehicle is modelled with discrete elements of mass, stiffness and damping. The full 3-D model of the vehicle which has been used in most of the simulations consists basically of carbody, and two identical bogies, each of them having two wheelsets. The wheels have a S1002 profile. All these bodies are represented with rigid masses, and are interconnected with different spring and damper elements, representing the primary and secondary suspensions. The complete model has 50 DOF.

The different simulations have also been carried out with simpler models of the vehicle, and the validity of the simplified models for the performed simulations has been analysed. In some of the performed simulations, the vehicle model is reduced either to a single wheelset with a static force equivalent to the nominal axle load of the vehicle acting on it, or to three equivalent masses (one for the wheelset, another for the bogie and another for the carbody) with equivalent vertical stiffness and damping elements between them representing the primary and secondary suspensions.

Numerical simulations of the vehicle running on straight track with vertical rail irregularities have been carried out with the models described in the previous section. The vehicle speed is 250 km/h for all the simulations presented here. Two types of rail irregularities have been considered as the vertical excitation input: a randomly distributed low frequency broadband rail irregularity on one hand, and a high frequency irregularity on the other hand. The low frequency broadband irregularity used corresponds to low intensity vertical rail irregularities, according to ERRI B 176 [22]. The high frequency excitation is defined according to the following PSD function taken from [8]:

$$G_V(f) = 0.036 f^{-3.15} \tag{4}$$

where the units of $G_v(f)$ are mm^2/(1/m), and f is the spatial frequency in cycle/m. This type of high frequency irregularitiy could represent a corrugated rail, which often provokes significant track vibrations and wheel-rail force fluctuations [23]. Wavelengths between 40 mm and 200 mm are considered for this second type of excitation.

5. COMPARISON OF RESULTS WITH DIFFERENT VEHICLE-TRACK MODELS

The simulations of the vehicle running on straight track with vertical rail irregularities have been carried out with the different vehicle-track models explained previously. In this section the results obtained with the different vehicle-track models are compared, and some conclusions are obtained in relation to the validity of the simpler vehicle-track models in some situations.

5.1. Comparison between the RMB, FE, and EMB models

Concerning the simulations with the low frequency broadband rail irregularity, comparable results are obtained with the simpler RMB and FEM vehicle-track models, and with the more complete EMB models, in the case of the ballasted, RHEDA 2000, and STEDEF tracks. In Figure 4 the results obtained with the different vehicle-track models for the case of the ballasted track are shown as an example.

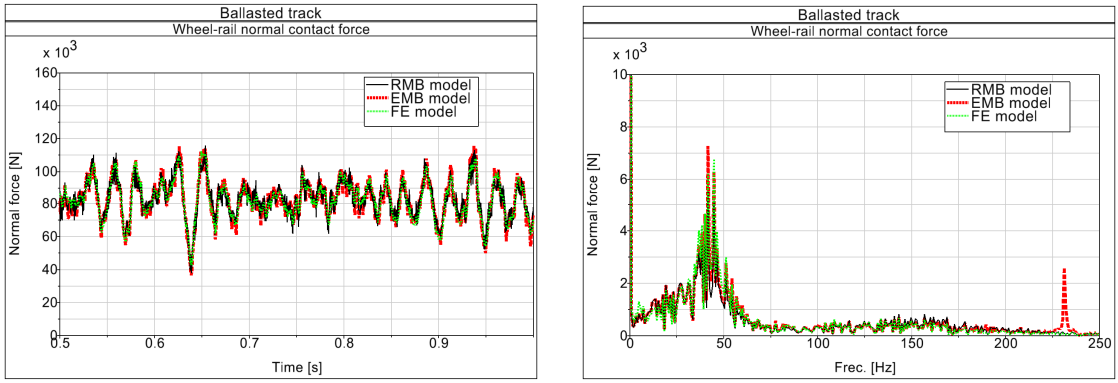

Fig. 4 Comparison of the results obtained for the wheel-rail contact force in the case of the ballasted track, with different vehicle-track models. Time history of the wheel-rail contact forces (left) and corresponding frequency spectra (right) with the low frequency broadband irregularity, obtained with the EMB (solid line), FE (dashed line), and RMB (dotted line) vehicle track models.

These results are justified because the conditions necessary for these simpler models to be valid are fulfilled: on one hand, the influence of the parametric excitation in these tracks is small compared to the influence of the rail roughness. On the other hand, the interaction between different wheelsets of the vehicle is small in this frequency range, because the only longitudinal coupling between them is provided by the rails, with a relatively low longitudinal stiffness. Lastly, the influence of the relative longitudinal motion of the vehicle with respect to the track is also negligible, because the wave propagating speeds at 25 Hz and above are much higher than the forward speed of the vehicle.

It is particularly remarkable the high similarity seen between the results obtained with the RMB models, and those obtained with the much more costly EMB models, despite the great difference of the track modelling in both cases. It has to be taken into account, however, that a parameter adjustment for the discrete track elements in the RMB models has been necessary. This is based on a previous frequency analysis of a FEM model of the track as mentioned previously, in order to approximate the results obtained with the EMB models. With a proper parameter adjustment, a very good correspondence of the receptance of the discrete assembly representing the track beneath each of the vehicle's wheelset, to the receptance calculated with full FEM models of the track, can be achieved. Consequently, the much simpler models of the track in the RMB models can approximate well the results obtained with the more detailed EMB models.

In the case of the floating slab track, however, different results are obtained with the different vehicle-track models. The reason is that in this case, the influence of the parametric excitation is much higher than in the other types of tracks, due to the fact that the sleeper passing frequency is close to the

frequency of the second vibration mode of the wheelset-track system which is easily excited at this frequency range. Also, in this case, the relative difference of the track receptance at different positions inside a sleeper bay is higher than in the other tracks, and this contributes to further increase the influence of the parametric excitation.

In Figure 5 the wheel-rail contact force calculated with the EMB vehicle-track models, for the vehicle running on each of the tracks with no irregularities is represented. Therefore, in this case, the only dynamic effect comes from the parametric excitation. This effect is seen to be much higher in the case of the floating slab than in the other tracks, as has been stated.

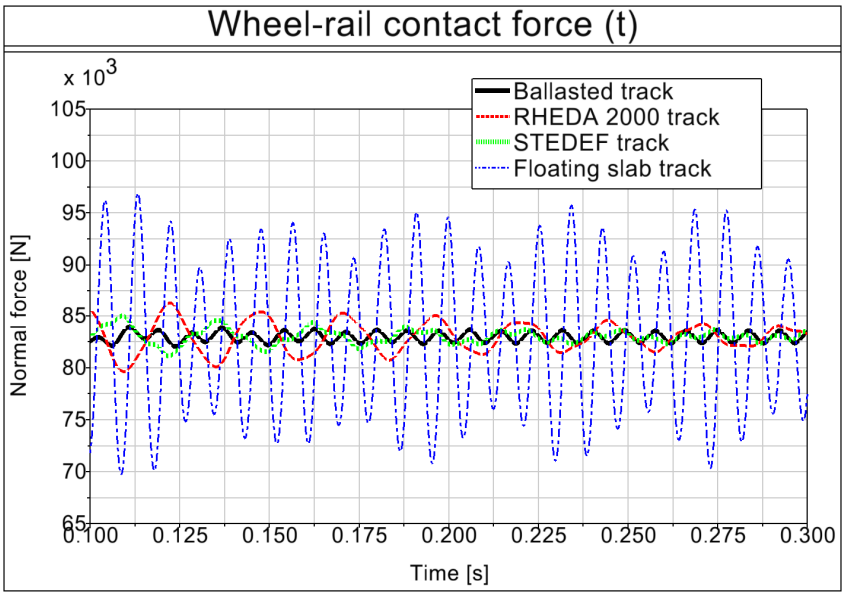

Fig. 5 Time history of the wheel-rail contact forces with no rail irregularities, for the ballasted (solid line), RHEDA 2000 (dashed line), STEDEF (dotted line), and floating slab tracks (dashed-dotted line). Results calculated with EMB vehicle-track models and full vehicle model

Concerning the simulations with the high frequency broadband rail irregularity, this time different results are obtained with the different models, as can be seen in Figure 6, in which the wheel-rail forces obtained with the different vehicle-track models for the STEDEF track are depicted, both in time and frequency domain. The results for the other track types are qualitatively similar.

The most different results compared to those of the EMB models are obtained with the RMB models. In these models, as it has been explained before, a reasonably good approximation of the track receptance can be obtained with the discrete assemblies representing the track beneath each wheelset, for frequencies up to a few hundred Hz. At high frequencies, however, the receptances of these discrete assemblies do not approximate well the receptances calculated with the complete FEM models of the tracks. The results obtained with the FEM vehicle-track models approximate better those obtained with the EMB models, but still some differences are noted between the results of both types of models. These differences are due to the differences in the track receptance at different points along each sleeper bay, which are greatest around the pinned-pinned resonance frequency. The FEM models cannot account for this variation in the track receptance, because the vehicle is static at one point in the track.

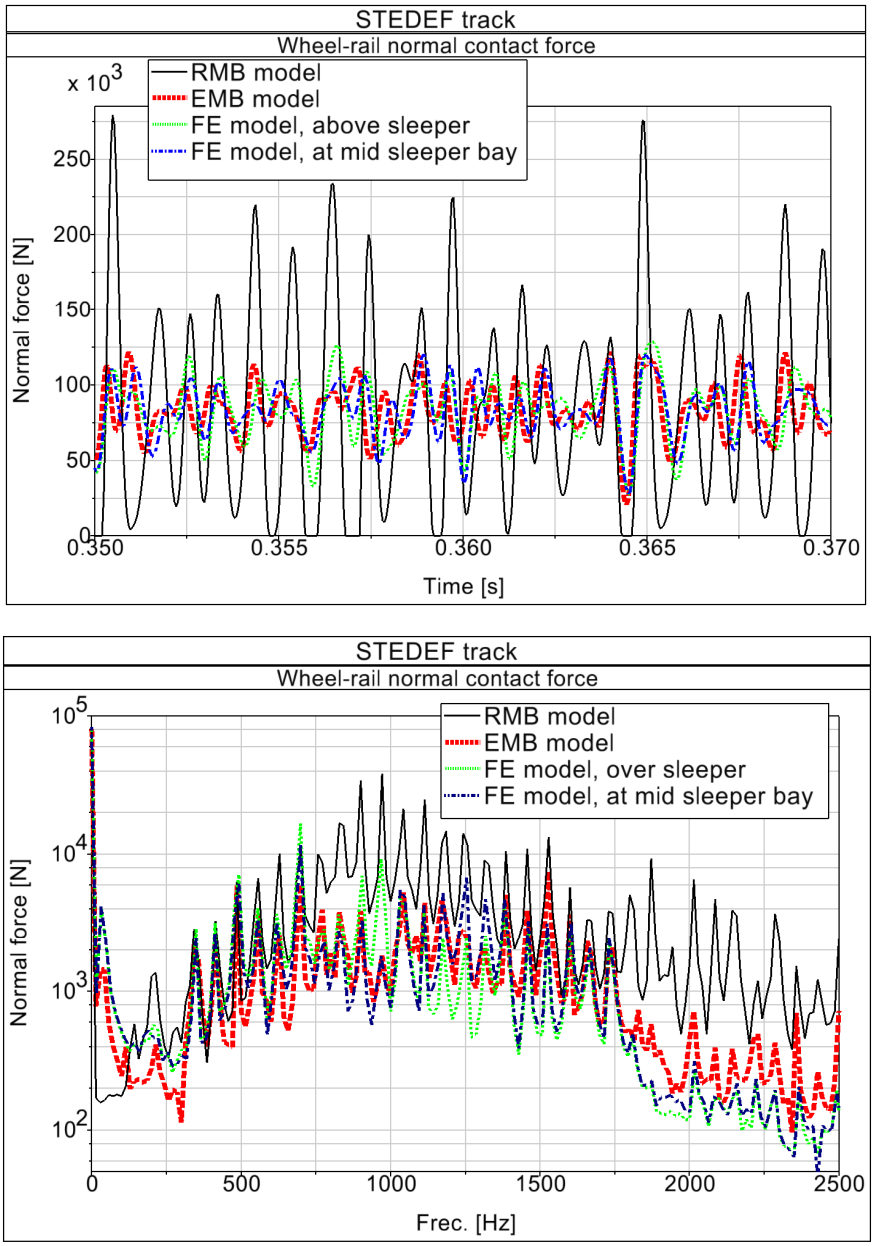

Fig. 6 Comparison of the results obtained for the wheel-rail contact force in the case of the STEDEF track, with different vehicle-track models. Time history of the wheel-rail contact forces (up figure) and corresponding frequency spectra (down figure) with the high frequency broadband irregularity, obtained with the EMB (solid line), FE (dashed line), and RMB (dotted line) vehicle track models

5.2. Comparison of models with single or multiple wheelsets

Concerning the simulations with the low frequency broadband rail irregularity, similar results are obtained in the simulations with a single or with multiple wheelsets, for the ballasted, RHEDA 2000 and STEDEF track, because, as has been previously discussed, the interaction between different wheelsets is small at low frequencies.

On the other hand, in the case of the floating slab track, similar results are also obtained with a single wheelset or with multiple wheelsets. In this case, the floating slab couples the different wheelsets of the vehicle with much higher longitudinal stiffness than the rails in the previous cases. However, this coupling only takes place at low frequencies, below the natural frequency of the slab vibrating above the elastic mat beneath it. At higher frequencies, the vibration of the rails is decoupled from the vibration of the slab. Although the vibrations of the slab are transmitted along a great distance in the track due to its

high longitudinal stiffness, the vibration levels seen in the slab at frequencies above the natural frequency of the slab are quite lower than those seen in the rails.

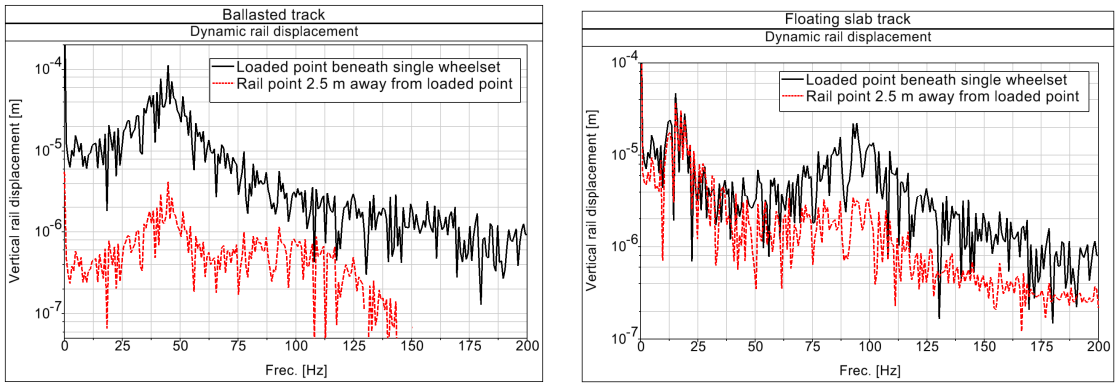

Fig. 7 Frequency spectra of the dynamic rail displacements of the rail obtained from simulations with the FEM vehicle-track models and with a single vehicle wheelset, at the point beneath the wheelset (solid line), and at the point where the other wheelset of the bogie would be (dashed line). Ballasted track (left) and floating slab track (right)

In Figure 7, the frequency spectra of the dynamic displacement of the rails is represented, obtained from simulations with a single vehicle wheelset. The displacements of the rail point beneath the vehicle's wheelset, and the displacements of the rail point where the other wheelset of the same bogie would have been, are represented for the case of the ballasted and floating slab tracks. The results for the other two types of track are qualitatively similar to those of the ballasted track. It can be seen that the displacements of the point where the other wheelset of the bogie would have been, are much smaller than the displacements beneath the modelled wheelset in the case of the ballasted track, at all frequencies. In the case of the floating slab track, this is also true at frequencies above and sufficiently separated from the slab's cut-on frequency. Below this frequency, the displacements of both points are similar. However, at these lower frequencies the wheel-rail contact forces are not being excited in this track, as will be seen in section 6.1. Therefore, Figure 7 clearly shows that the dynamic interaction between the different wheelsets of the vehicle is small for the studied track types with the low frequency broadband rail irregularity considered.

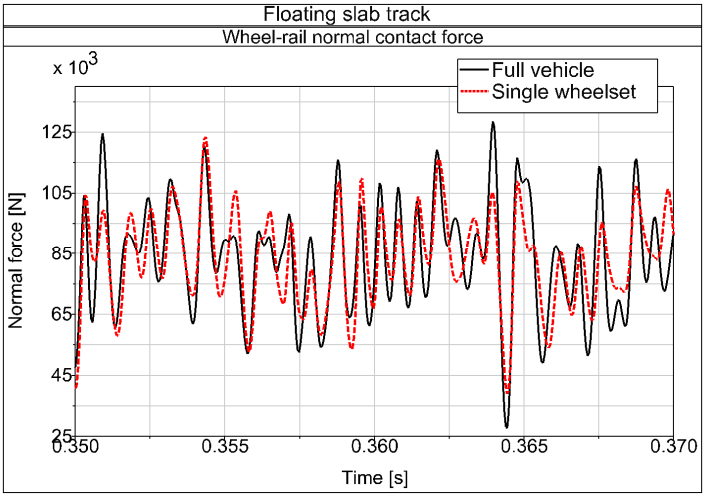

Fig. 8 Comparison of the results obtained for the wheel-rail contact force in the case of the floating slab track, with a single or with multiple wheelsets. Time history of the wheel-rail contact forces with the high frequency broadband irregularity, obtained with the full model of the vehicle (solid line), and with the simplified model of the vehicle consisting of a single wheelset with a static force applied on it (dashed line)

In the case of the simulations with the high frequency broadband rail irregularity, some differences can be seen between the results obtained with one, or with multiple wheelsets, because at high frequencies the dynamic interaction between different wheelsets through the rails is not negligible. Figure 8 shows as an example the comparison of the wheel-rail contact forces obtained for the floating slab track with the EMB vehicle-track models, with a single, or with multiple wheelsets, in the time domain (the differences seen in the frequency domain are much smaller).

Nevertheless, as seen in Figure 8, only moderate differences in the wheel-rail contact forces are noted in the time domain, but the amplitude and the frequency content of the force oscillations is very similar with one or with multiple wheelsets. Therefore, in many applications a single wheelset model can provide quite accurate results of the vehicle-track interaction.

5.3. Comparison of 1-D and 3-D mesh for the slab in the floating slab track

In the case of the FE and EMB vehicle-track models of the floating slab track, both 1-D and 3-D meshings for the slab have been considered.

Figure 9 shows the time history of the vertical displacements of three points of the slab, during a bogie passage in the case of the floating slab track with 3-D slab meshing. The three points considered belong to the same vertical plane of the slab, and are located at different lateral distances from the track centre. It can be seen that the vibration of the slab in both cases is fundamentally one-dimensional in the vertical direction, since the displacements of different points across its width are very similar.

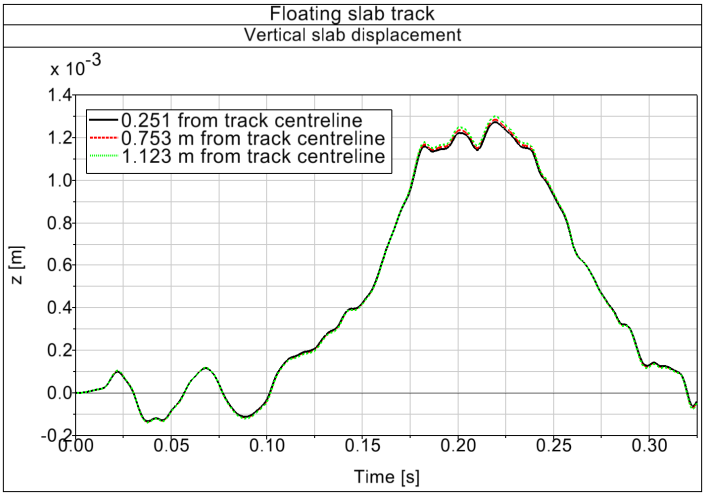

Fig. 9 Vertical displacement of the slab in the floating slab track model, with 3-D meshing of the slab

In order to further check the validity of the 1-D meshing of the slab, FE models of the full floating slab track have been constructed, using both the 1-D and the 3-D meshings for the slab, and their receptances have been calculated with NASTRAN in a frequency range from 0 to 2500 Hz. Although not shown here, the receptances calculated with the much simpler 1-D meshings for the slab show very good agreement with those calculated with the 3-D slab meshings, in the whole frequency range. Therefore, it can be concluded that a 1-D representation of the slab is suitable for vehicle-track interaction studies, and that the much more costly 3-D meshing does not bring any additional characteristic not already discerned by the 1-D meshing.

5.4. Comparison of computational costs

In Figure 10 the computation times with different types of vehicle-track models are compared (note the logarithmic scale). The EMB models have the highest computational costs. The computational costs of the FE and RMB models are much lower, and of the same order, although it has to be said that their relative computational costs can vary substantially, depending, for example, on the number of degrees of freedom of each model, or on the type of wheel-rail contact model used. Within the EMB models, the computation times can also vary substantially, depending on the degree of detail with which the elastic bodies are represented.

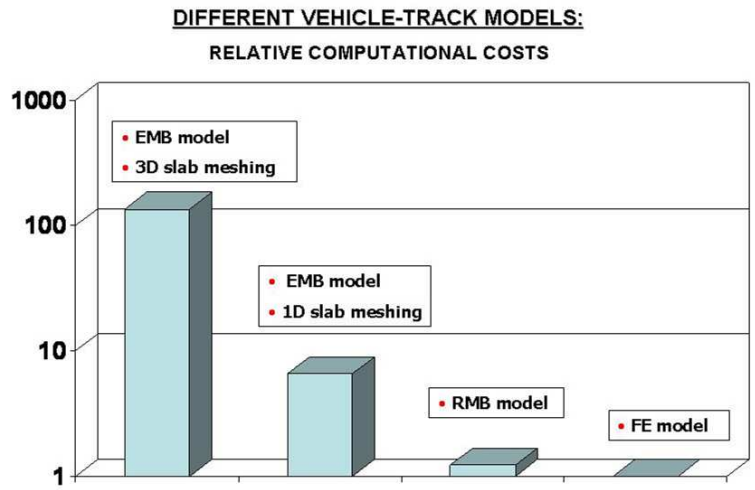

Fig. 10 Comparison of computational costs with different vehicle-track models.

6. RESULTS AND DISCUSSION

In this section, the results obtained for the different track types studied are presented, with two types of broadband vertical rail irregularities as described previously, at low and at high frequencies. All the results presented in this section have been obtained with the EMB vehicle-track models, and the complete model of the vehicle.

6.1 Wheel-rail contact forces

Figure 11 shows the time history and the corresponding frequency spectra of the wheel-rail contact force for the different track types studied, with the low frequency broadband vertical rail irregularity.

Fluctuations in the wheel-rail contact force are clearly larger in the RHEDA 2000 and floating slab tracks than in the ballasted and STEDEF tracks. In these two last tracks, the first natural mode of the tracks, in which the sleepers vibrate in phase with the rails, is being excited. In the RHEDA 2000 track as well, the first natural mode of the track is the one which is most excited. In this mode, rails and base plates vibrate in phase above the lower elastic base plate pad. In the case of the floating slab track, the second mode of the track is being excited, in which the rails vibrate out of phase with the slab.

In all four tracks, the frequencies at which peaks occur in the frequency spectra of the wheel-rail contact forces match well with the frequencies of the corresponding natural vibration modes of the track calculated analytically from equivalent 2 DOF systems, similar to the ones that are employed to model the track in the RMB models as described previously. In order to calculate these frequencies, the mass of the wheelset is added to the mass of the elastic level representing the rails, in order to properly account for the vibration of the whole vehicle-track system.

For the case of the high frequency broadband vertical rail irregularity, Figure 12 shows the time history and the corresponding frequency spectra of the wheel-rail contact force for the different track types studied.

In this case, the obtained results for the wheel-rail contact forces are very similar for the ballasted track, STEDEF track and floating slab track. For these tracks, only significant differences are seen in the contact force spectra at frequencies related to the vibration modes of the different tracks and at the sleeper passing frequency. On the contrary, for the RHEDA 2000 track differences in the wheel-rail forces are also noted at higher frequencies. In order to explain this result, the receptances of the different tracks are compared in Figure 13.

It is seen that for the ballasted, STEDEF and floating slab tracks, for frequencies above about 500 Hz, once the different resonance frequencies of the tracks have been passed, the receptances are very similar. In these tracks the receptances at high frequencies converge to that of the unsupported free rail (with the exception of the pinned-pinned resonance, characteristic of a discretely supported rail). In the case of the RHEDA 2000 track, the high frequency eigenmode related with the stiff rail pad between the rail and the light base plate alters the track receptance at higher frequencies. Additionally, in this track the pinned-

pinned resonance happens at a slightly lower frequency than in the other tracks, due to the higher sleeper spacing (see Table 1).

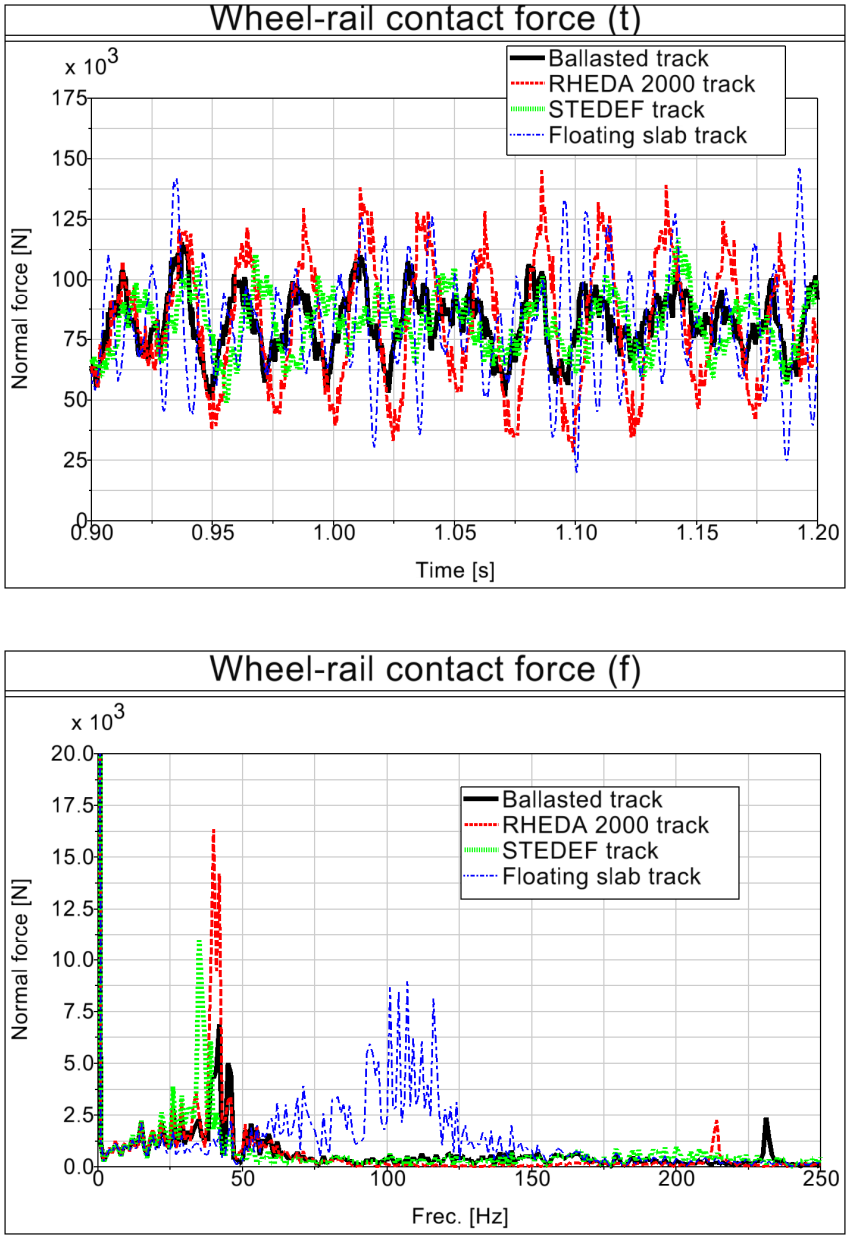

Fig. 11 Time history of the wheel-rail contact forces (up figure) and corresponding frequency spectra (down figure) with the low frequency broadband irregularity, for the ballasted (solid line), RHEDA 2000 (dashed line), STEDEF (dotted line), and floating slab tracks (dashed-dotted line).

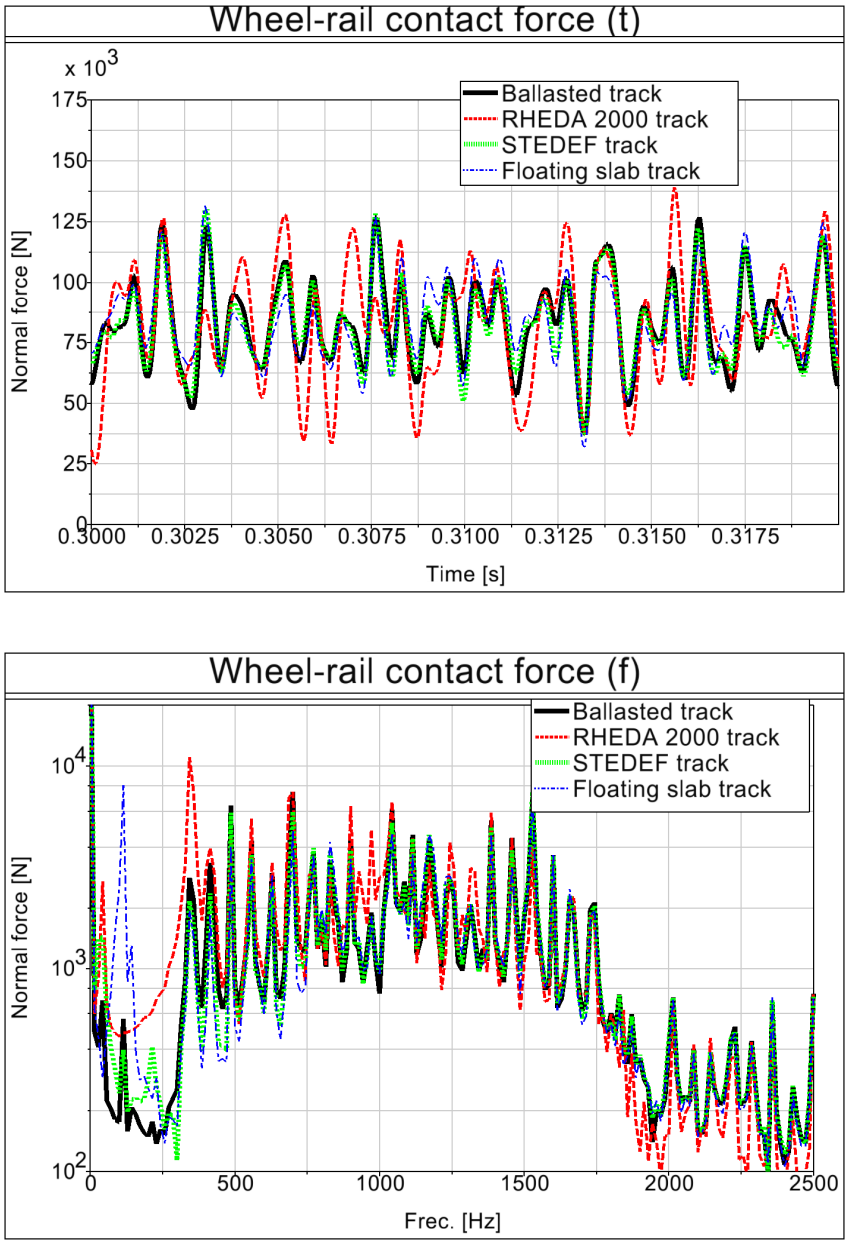

Fig. 12 Time history of the wheel-rail contact forces (up figure) and corresponding frequency spectra (down figure) with the high frequency broadband irregularity, for the ballasted (solid line), RHEDA 2000 (dashed line), STEDEF (dotted line), and floating slab tracks (dashed-dotted line)

6.2 Pad forces

In this section, the pad forces obtained with the different types of tracks studied are compared, for the two types of irregularities considered, i.e. the low frequency broadband irregularity and the high frequency broadband irregularity.

Figure 14 shows the pad forces obtained for each type of track during a vehicle passage with low frequency broadband rail irregularity. For each type of track the pad with the highest dynamic force is depicted.

The pad forces obtained in the floating slab track are much larger than those obtained in the other types of track studied. In this track, a much lower degree of rail bending is allowed, due to the high stiffness of the rail pad and the slab. As a result, the number of pads sharing the vehicle load at any given time is reduced, and the peak value of the force seen by each pad is increased.

In Figure 15, the pad forces obtained for each type of track during a vehicle passage with the high frequency broadband rail irregularity are shown.

Similar tendencies to the ones observed with the low frequency rail irregularity are seen also with the high frequency rail irregularity when comparing the peak forces seen in each type of track.

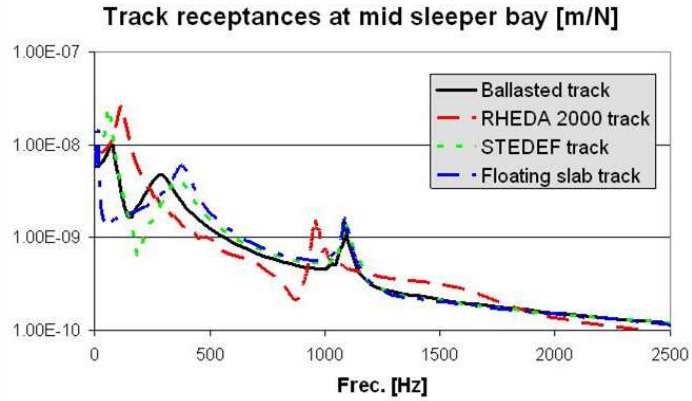

Fig. 13 Comparison of the track receptances, for the ballasted (solid line), RHEDA 2000 (dashed line), STEDEF (dotted line), and floating slab tracks (dashed-dotted line)

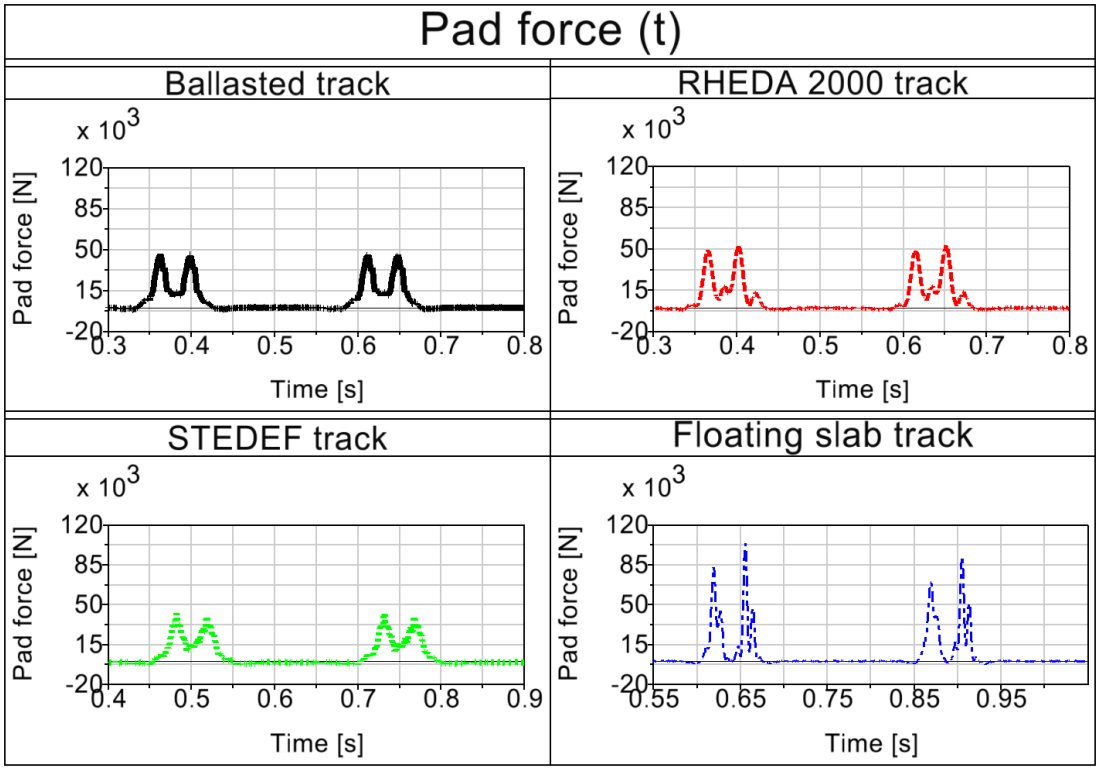

Fig. 14 Time history of the pad forces with the low frequency broadband irregularity, for the ballasted (solid line), RHEDA 2000 (dashed line), STEDEF (dotted line), and floating slab tracks (dashed-dotted line)

The slightly larger pad force seen in the RHEDA 2000 track compared to the ballasted and STEDEF tracks is justified because in this track the number of rail pads per sleeper length considered is lower than in the other tracks. In the case of this track, the force in the upper stiff rail pad has been plotted. In Figure 16 the forces in the upper stiff rail pad and in the lower flexible base plate pad are compared. Obviously, the high frequency content in the lower base plate pad is much lower, as it is filtered by the base plate.

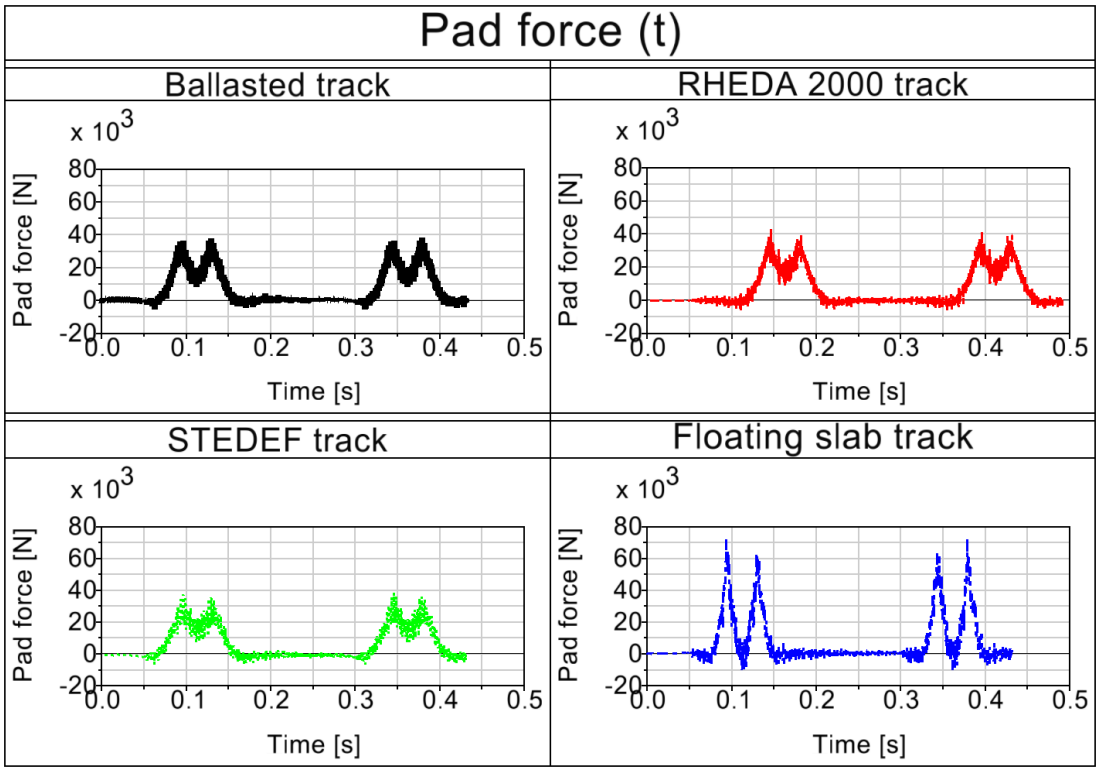

Fig. 15 Time history of the pad forces with the high frequency broadband irregularity, for the ballasted (solid line), RHEDA 2000 (dashed line), STEDEF (dotted line), and floating slab tracks (dashed-dotted line)

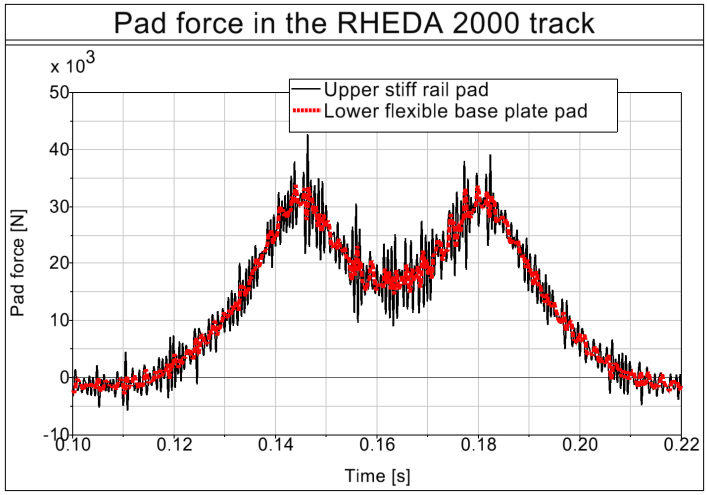

Fig. 16 Comparison of the forces in the upper stiff rail pad and lower flexible base plate pad in the RHEDA 2000 track

7. CONCLUSIONS

The dynamic performance of a high speed ballasted track and three different types of slab tracks has been studied by means of numerical simulations in the time domain of a vehicle running on a straight section of track at high speed with vertical rail irregularities. Different types of vehicle-track models have been constructed in order to study the vertical dynamic vehicle-track interaction, and a comprehensive representation of the whole vehicle-track system, necessary for the study of dynamic phenomena at high

frequencies, has been achieved making use of systematic methodologies and standard tools offered in a commercial MBS and in a commercial FEM analysis tool.

The conclusions obtained with respect to the comparison of the dynamic performance of the different types of track studied, and with respect to the validity of the results obtained with the different types of vehicle-track models used, as well as the most adequate configuration of those models, are summarized below.

As mentioned previously, the different results have been obtained considering a single set of typical physical parameters for each of the tracks, but some of the parameters, e.g. the pad stiffness, and consequently the dynamic properties of the tracks, can change within a certain range. Consequently the conclusions obtained must not be generalized straightforwardly to other possible configurations of each type of track. The conclusions obtained are as follows:

- The wheel-rail contact forces have a lower degree of fluctuations in the ballasted track and in the STEDEF track, than in the other two types of slab tracks studied (RHEDA 2000 and floating slab). In the case of the floating slab track, although vibration transmission to the ground is expected to be considerably reduced, vibration levels between the loading source and the slab may be enlarged, as pointed out by other authors [3].
- The pad forces in the floating slab track are much higher than in the other tracks studied, due to the low degree of rail bending allowed by the stiffness of both pad and slab, which prevents the load of the vehicle from being more effectively spread between more pads along the track.
- In the studied design of floating slab track, another problem is seen for high speed applications: the effect of the parametric excitation is much higher than in the other studied track types, implying that even for smooth railhead and wheel surfaces, a considerable degree of fluctuations is already seen in the wheel-rail contact forces.
- At low and mid frequencies, up to a few hundred Hz, and when the effects of the parametric excitation are not important, very simple, full FE models of the vehicle-track system, with the wheel-rail contact condition simplified to a linear spring, are seen to be entirely satisfactory for the study of vertical vehicle-track dynamics.
- Additionally, in the case of tracks without a floating slab or tracks with a floating slab in which the dominant wheel-rail vibration takes place at frequencies much higher than the slab cut-on frequency, the interaction between different wheelsets of the vehicle is seen to be very small at frequencies up to a few hundred Hz.

  In these cases, the track models may be further simplified to discrete spring-damper-mass assemblies beneath each wheelset with very few degrees of freedom. The results obtained with these simple models match very well with those obtained with more complex track models, if the physical parameters of mass, stiffness and damping of the discrete track elements are carefully chosen adjusting the receptance of the Rigid Multibody track to that of the actual flexible track. Also, a very simple model of the vehicle may be used for the study of wheel-rail contact forces in these cases, consisting of a single wheelset with a static load applied on it.
- Modelling the elasticity of the slab in slab tracks significantly increases the complexity of vehicle-track models. Although mathematical procedures have been developed that enable a very detailed modelling of the slab as an elastic plate, in this work it is found that a much simpler modelling of the slab by means of 1-D beam elements, is entirely satisfactory to study dynamic phenomena even at high frequencies, as it has been shown that the slab vibrates fundamentally in the vertical plane. With the simpler 1-D beam model of the slab, the computational costs of the model are greatly reduced.

ACKNOWLEDGEMENTS

The authors wish to thank the Spanish Ministry of Development and the Ministry of Science and Innovation for the finance received through T 83/2006 and TRA 2010-18386 research projects. The authors also acknowledge the financial help received from the Department of Education, Universities and Research of the Basque Government through IT-453-10.

REFERENCES

[1] **Lombaert, G., G. Degrande, B. Vanhauwere, B. Vandeborght,** and **S. François.** The control of ground-borne vibrations from railway traffic by means of continuous floating slabs. *J. Sound Vibrat.*, 2006, **297**, 946-961.

[2] **Hussein, M. F. M.** and **H. E. M. Hunt.** Modelling of floating-slab tracks with continuous slabs under oscillating moving loads. *J. Sound Vibrat.*, 2006, **297**, 37-54.

[3] **Kuo, C., C. Huang,** and **Y. Chen.** Vibration characteristics of floating slab track. *J. Sound Vibrat.*, 2008, **317**, 1017-1034.

[4] **Wu, T. X.** and **D. J. Thompson.** On the parametric excitation of the wheel/track system. *J. Sound Vibrat.*, 2004, **278**, 725-747.

[5] **Xie, G.** and **S. D. Iwnicki.** Simulation of wear on a rough rail using a time-domain wheel–track interaction model. *Wear*, 2008, **265**, 1572-1583.

[6] **Otero, J., Martínez, J.,** and **de los Santos, M.A.** Evaluación de las vibraciones generadas al paso de un tren considerando diferentes tipologías de vía. *9º Congreso Iberoamericano de Ingeniería Mecánica*, 2009.

[7] **Jin, X., X. Xiao, Z. Wen,** and **Z. Zhou.** Effect of sleeper pitch on rail corrugation at a tangent track in vehicle hunting. *Wear* , 2008, **265**, 1163-1175.

[8] **Zhai, W., K. Wang,** and **C. Cai.** Fundamentals of vehicle-track coupled dynamics. *Veh. Syst. Dyn.*, 2009, **47**, 1349-1376.

[9] **Nielsen, J. C. O., R. Lunden, A. Johansson,** and **T. Vernersson.** Train-track interaction and mechanisms of irregular wear on wheel and rail surfaces. *Veh. Syst. Dyn.*, 2003, **40**, 3-54.

[10] **Popp, K., K. Knothe,** and **C. Popper.** System dynamics and long-term behaviour of railway vehicles, track and subgrade: report on the DFG priority programme in Germany and subsequent research. *Veh. Syst. Dyn.*, 2005, **43**, 485-538.

[11] **Popp, K., H. Kruse, and I. Kaiser.** Vehicle-track dynamics in the mid-frequency range. *Veh. Syst. Dyn.*, 1999, **31**, 423-464.

[12] **Knothe, K. L.** and **S. L. Grassie.** Modeling of Railway Track and Vehicle Track Interaction at High-Frequencies. *Veh. Syst. Dyn.*, 1993, **22**, 209-262.

[13] **Dietz, S., G. Hippman,** and **G. Schupp.** Interaction of vehicle and flexible tracks by co-simulation of multibody vehicle systems and finite element track models. *Veh. Syst. Dyn.*, 2002, **37**, 372-384.

[14] **Bezin, Y., S. D. Iwnicki, M. Cavalletti, E. de Vries, F. Shahzad,** and **G. Evans.** An investigation of sleeper voids using a flexible track model integrated with railway multi-body dynamics. *Proc. IMechE, Part F: J. Rail and Rapid Transit*, 2009, **223**, 597-607.

[15] **Bezin, Y., D. Farrington, C. Davies, C. Penny, B. Temple, E. Kassa,** and **S. D. Iwnicki.** The dynamic response of a slab track construction and its benefits with respect to conventional ballasted track. In Proceedings of the 21st International Symposium on Dynamics of Vehicles on Roads and Tracks, Stockholm, Sweeden, 17-21 August 2009 (KTH Royal Institute of Technology, Stockhom).

[16] **Gonzalez, F. J., B. Suarez, J. Paulin,** and **I. Fernandez.** Safety assessment of underground vehicles passing over highly resilient straight track in the presence of a broken rail. *Proc. IMechE, Part F: J. Rail and Rapid Transit*, 2008, **222**, 69-84.

[17] **Vossloh Fastening Systems.** www.vossloh-fastening-systems.de. **2010**.

[18] **SIMPACK GmbH.** SIMPACK Wheel Rail Element Reference., 2007.

[19] **Herting, D. N.** The MSC/NASTRAN Advanced Dynamic Analysis User's Guide, version 7. 2004.

[20] **Guyan, R.J.** Reduction of Stiffness and Mass Matrices. *AIAA Journal*, 1965, **3**, 380.

[21] **Baeza, L., A. Roda,** and **J. C. O. Nielsen.** Railway vehicle/track interaction analysis using a modal substructuring approach. *J. Sound Vibrat.* , 2006, **293**, 112-124.

[22] **ERRI:B176/3.** Benchmark problem - results and assesment. *B176/DT290* , 1993.

[23] **Oyarzabal, O., J. Gomez, J. Santamaria,** and **E. G. Vadillo.** Dynamic optimization of track components to minimize rail corrugation. *J. Sound Vibrat.*, 2009, **319**, 904-917.

APPENDIX

Notation

C_H	Hertzian wheel-rail contact constant
f	spatial frequency
F	static normal wheel-rail force
$f_{p,k}$	force of the kth railpad in an elastic rail
$f_{wr,j}(t)$	wheel-rail force at the jth wheel in an elastic rail
$G_v(f)$	power spectral density function of rail roughness
k_H	linearized wheel-rail contact stiffness
m	number of wheelsets
m_i	generalized mass of the ith mode of an elastic rail
n	number of railpads
N	normal wheel-rail force
u_R	one degree of freedom of an elastic rail
x	longitudinal coordinate of track
$x_{p,k}$	longitudinal coordinate along the rail of the jth railpad
$x_{w,j}$	longitudinal coordinate along the rail of the jth wheel
$z_i(t)$	modal displacement of the ith mode of an elastic rail
ξ_i	damping ration of the ith mode of an elastic rail
$\Phi_i(x)$	shape function of the ith mode of an elastic rail
ω_i	natural frequency of the ith mode of an elastic rail